Quantum Nondemolition Measurement of Large-Spin Ensembles by Dynamical Decoupling

M. Koschorreck,[1,*] M. Napolitano,[1] B. Dubost,[1,2] and M. W. Mitchell[1]

[1]*ICFO-Institut de Ciencies Fotoniques, 08860 Castelldefels (Barcelona), Spain*

[2]*Laboratoire Matériaux et Phénomènes Quantiques, Université Paris Diderot et CNRS, UMR 7162, Bât. Condorcet, 75205 Paris Cedex 13, France*

(Received 17 May 2010; revised manuscript received 26 July 2010; published 25 August 2010)

Quantum nondemolition (QND) measurement of collective variables by off-resonant optical probing has the ability to create entanglement and squeezing in atomic ensembles. Until now, this technique has been applied to real or effective spin one-half systems. We show theoretically that the buildup of Raman coherence prevents the naive application of this technique to larger spin atoms, but that dynamical decoupling can be used to recover the ideal QND behavior. We experimentally demonstrate dynamical decoupling by using a two-polarization probing technique. The decoupled QND measurement achieves a sensitivity 5.7(6) dB better than the spin projection noise.

DOI: 10.1103/PhysRevLett.105.093602 PACS numbers: 42.50.Lc, 03.67.Bg, 07.55.Ge, 42.50.Dv

Quantum nondemolition measurement plays a central role in quantum networking and quantum metrology for its ability to simultaneously detect and generate nonclassical quantum states. The original proposal by Braginsky [1] in the context of gravitational wave detection has been generalized to the optical [2,3], atomic [4] and nanomechanical [5] domains. In the atomic domain, QND by dispersive optical probing of spins or pseudospins has been demonstrated using ensembles of cold atoms on a clock transition [6,7], and with polarization variables [8,9], but thus far only with real or effective spin-1/2 systems.

QND measurement of larger spin systems offers a metrological advantage, e.g., in magnetometry [10], and may be essential in novel proposals for quantum polarization spectroscopy in spinor gases and the detection of exotic quantum phases that intrinsically rely on large-spin systems [11–13]. Dispersive interactions with large-spin atoms are complicated by the presence of non-QND-type terms in the effective Hamiltonian describing the interaction [14–16]. As we show in agreement with [17,18], these terms prevent a pure QND measurement [1] for large-spin ensembles even in the large-detuning limit, once considered free from the problem [19]. The non-QND terms introduce noise into the measured variable, or equivalently decoherence into the atomic state. The problem is serious for both large and small ensembles, so that conventional (naive) application of dispersive probing fails for several of the above-cited proposals. Composite systems of two ensembles have demonstrated cancellation of the non-QND effects [20]. In contrast, we show how non-QND terms can selectively be turned off, to allow a pure QND measurement of a true large-spin system.

We approach this problem using the methods of dynamical decoupling [21–23], which allow us to effectively cancel the non-QND terms in the Hamiltonian while retaining the QND term. To our knowledge, this is the first application of this method to quantum nondemolition measurements. Dynamical decoupling has been extensively applied in magnetic resonance [24,25], used to suppress collisional decoherence in a thermal vapor [26], to extend coherence times in solids [27], in Rydberg atoms [28], and with photon polarization [29]. Other approaches include application of a static perturbation [17,30].

We consider an ensemble of spin-f atoms interacting with a pulse of near-resonant polarized light. As described in Refs. [14–16], the light and atoms interact by the effective Hamiltonian $\hat{H}_{\mathrm{eff}}$

$$\tau\hat{H}_{\mathrm{eff}} = G_1\hat{S}_{\mathbf{z}}\hat{J}_{\mathbf{z}} + G_2(\hat{S}_{\mathbf{x}}\hat{J}_{\mathbf{x}} + \hat{S}_{\mathbf{y}}\hat{J}_{\mathbf{y}}), \tag{1}$$

where τ is the duration of the pulse and $G_{1,2}$ are coupling constants that depend on the atomic absorption cross section, the beam geometry, the detuning from resonance Δ, and the hyperfine structure of the atom [31]. The atomic variables $\hat{\mathbf{J}}$ (described below) are collective spin and alignment operators. The light is described by the Stokes operators $\hat{\mathbf{S}}$ defined as $\hat{S}_i \equiv \frac{1}{2}(\hat{a}_+^\dagger, \hat{a}_-^\dagger)\sigma_i(\hat{a}_+, \hat{a}_-)^T$, where the σ_i are the Pauli matrices and $\hat{a}_\pm$ are annihilation operators for the temporal mode of the pulse and circular plus or minus polarization. Bold subscripts, e.g., $\mathbf{x}$, are used to label nonspatial directions for atomic and light variables. The G_1 term describes a QND interaction, while the G_2 describes a more complicated coupling. In the dispersive, i.e., far-detuned, regime, G_1 and G_2 scale as Δ^{-1} and Δ^{-2}, respectively. It has sometimes been assumed that the G_2 terms can be neglected for sufficiently large Δ, leaving an approximate QND interaction. As we show below, this scaling argument fails, and the G_2 terms remain important. We note an important symmetry: $\hat{H}_{\mathrm{eff}}$ commutes with $\hat{S}_{\mathbf{z}} + \hat{J}_{\mathbf{z}}$, and is thus invariant under simultaneous rotation of $\hat{\mathbf{J}}$ and $\hat{\mathbf{S}}$ about the z axis.

The atomic collective variables are $\hat{J}_k \equiv \sum_i^{N_A}\hat{j}_k^{(i)}$ where the superscript indicates the ith atom and $\hat{j}_{\mathbf{x}} \equiv (\hat{f}_x^2 - \hat{f}_y^2)/2$, $\hat{j}_{\mathbf{y}} \equiv (\hat{f}_x\hat{f}_y + \hat{f}_y\hat{f}_x)/2$, $\hat{j}_{\mathbf{z}} \equiv \hat{f}_z/2$ and $\hat{j}_{[\mathbf{x},\mathbf{y}]} \equiv -i[\hat{j}_{\mathbf{x}}, \hat{j}_{\mathbf{y}}] = \hat{f}_z(\hat{f}^2 - \hat{f}_z^2 - 1/2)$. These obey commutation relations $[\hat{j}_{\mathbf{z}}, \hat{j}_{\mathbf{x}}] = i\hat{j}_{\mathbf{y}}$, $[\hat{j}_{\mathbf{y}}, \hat{j}_{\mathbf{z}}] = i\hat{j}_{\mathbf{x}}$, $[\hat{j}_{\mathbf{x}}, \hat{j}_{\mathbf{y}}] = i\hat{j}_{[\mathbf{x},\mathbf{y}]}$. For

$f = 1/2$, $\hat{j}_{\mathbf{x}}$, $\hat{j}_{\mathbf{y}}$ and $\hat{j}_{[\mathbf{x},\mathbf{y}]}$ vanish identically while for $f = 1$, $\hat{j}_{[\mathbf{x},\mathbf{y}]} = \hat{j}_{\mathbf{z}}$ so that $\hat{j}_{\mathbf{x}}$, $\hat{j}_{\mathbf{y}}$, and $\hat{j}_{\mathbf{z}}$ describe a pseudospin $\hat{\mathbf{j}}$.

In the QND scenario, an initial coherent polarization state with $\langle\hat{\mathbf{S}}\rangle = (N_L/2, 0, 0)$ is passed through the ensemble and experiences a rotation due to the G_1 term such that the component $\hat{S}_{\mathbf{y}}$ (the "meter" variable) indicates the value of $\hat{J}_{\mathbf{z}}$ (the "system" variable). We assume that $\langle\hat{J}_{\mathbf{x}}\rangle = N_A/2$. For a weak pulse, i.e., for $\langle\hat{\mathbf{S}}\rangle$ sufficiently small, we have the τ-linear input-output relations $\hat{A}^{(\mathrm{out})} = \hat{A}^{(\mathrm{in})} - i\tau[\hat{A}^{(\mathrm{in})}, \hat{H}_{\mathrm{eff}}]$. Of specific interest are

$$\hat{J}_{\mathbf{z}}^{(\mathrm{out})} = \hat{J}_{\mathbf{z}}^{(\mathrm{in})} + G_2\hat{S}_{\mathbf{x}}\hat{J}_{\mathbf{y}}^{(\mathrm{in})} - G_2\hat{S}_{\mathbf{y}}^{(\mathrm{in})}\hat{J}_{\mathbf{x}}, \tag{2}$$

$$\hat{J}_{\mathbf{y}}^{(\mathrm{out})} = \hat{J}_{\mathbf{y}}^{(\mathrm{in})} - G_1\hat{S}_{\mathbf{z}}^{(\mathrm{in})}\hat{J}_{\mathbf{x}} - G_2\hat{S}_{\mathbf{x}}\hat{J}_{[\mathbf{x},\mathbf{y}]}^{(\mathrm{in})}, \tag{3}$$

$$\hat{S}_{\mathbf{y}}^{(\mathrm{out})} = \hat{S}_{\mathbf{y}}^{(\mathrm{in})} + G_1\hat{S}_{\mathbf{x}}\hat{J}_{\mathbf{z}}^{(\mathrm{in})} - G_2\hat{S}_{\mathbf{z}}^{(\mathrm{in})}\hat{J}_{\mathbf{x}}, \tag{4}$$

which describe the change in the system variable, its conjugate, and the meter variable. In the case of $f = 1/2$, the G_2 terms vanish identically and we have a pure QND measurement: information about $\hat{J}_{\mathbf{z}}$ enters $\hat{S}_{\mathbf{y}}$ and there is a backaction on $\hat{J}_{\mathbf{y}}$, but not on $\hat{J}_{\mathbf{z}}$. The input noise $\mathrm{var}(\hat{S}_{\mathbf{y}}^{(\mathrm{in})}) = S_{\mathbf{x}}/2$ limits the performance of the measurement, and corresponds to a spin sensitivity of $\delta\hat{J}_{\mathbf{z}}^2 = (2G_1^2\hat{S}_{\mathbf{x}})^{-1}$. For comparison, the projection noise of an $\mathbf{x}$-polarized spin state is $\mathrm{var}(\hat{J}_{\mathbf{z}}) = J_{\mathbf{x}}/2$, so that projection noise sensitivity is achieved for $\hat{S}_{\mathbf{x}} = (G_1^2\hat{J}_{\mathbf{x}})^{-1} \equiv S_{\mathrm{SNR}}$.

This ideal QND regime does not occur naturally except for $f = 1/2$. In the interesting regime $\hat{S}_{\mathbf{x}} \approx S_{\mathrm{SNR}}$, we find that $G_2\hat{S}_{\mathbf{x}}\hat{J}_{\mathbf{y}} \approx \hat{J}_{\mathbf{y}}(G_2/G_1^2)\hat{J}_{\mathbf{x}}$ is independent of Δ, and cannot be neglected based on detuning. To get an order of magnitude, we note that for large detuning, $G_1 \approx \sigma_0\Gamma/4A\Delta$, $G_2 \approx G_1\Delta_{\mathrm{HFS}}/\Delta$ where σ_0 is the on-resonance scattering cross section, A is the effective area of the beam, and Γ and Δ_{HFS} are the natural linewidth and hyperfine splitting, respectively, of the excited states. In terms of the on-resonance optical depth $d_0 \equiv \sigma_0 N_A/A$, we find $G_2/G_1^2 J_{\mathbf{x}} \approx 8\Delta_{\mathrm{HFS}}/d_0\Gamma$. In a typical experiment with rubidium on the D_2 line, $\Delta_{\mathrm{HFS}}/\Gamma \sim 30$ and $d_0 \sim 50$ [31], so the contribution of this term is important.

In contrast, the last term in Eq. (2) and (4), respectively, contribute variances $\langle G_2^2\hat{S}_{\mathbf{y}}^2\hat{J}_{\mathbf{x}}^2\rangle$ and $\langle G_2^2\hat{S}_{\mathbf{z}}^2\hat{J}_{\mathbf{x}}^2\rangle$ which scale as Δ^{-2}. We will henceforth drop these terms.

The system variable $\hat{J}_{\mathbf{z}}$ is coupled to a degree of freedom, $\hat{J}_{\mathbf{y}}$, which is neither system nor meter in the QND measurement. This coupling introduces noise into the system variable, and decoherence into the state of the ensemble. To remove the decoherence associated with this coupling $G_2\hat{S}_{\mathbf{x}}\hat{J}_{\mathbf{y}}$, we adopt the strategy of "bang-bang" dynamical decoupling [21–23]. In this method, a unitary $\hat{U}_b$ and its inverse $\hat{U}_b^\dagger$ are alternately and periodically applied to the system p times during the evolution, so that the total evolution is $[\hat{U}_b^\dagger\hat{U}_H(t/2p)\hat{U}_b\hat{U}_H(t/2p)]^p$ where $\hat{U}_H(t)$ describes unitary evolution under $\hat{H}$ for a time t. With this evolution, those system variables that are unchanged by $\hat{U}_b$ continue to evolve under $\hat{H}$, while others are rapidly switched from one value to another, preventing coherent evolution. For large p, the system evolves under a modified Hamiltonian $\hat{H}' = \hat{P}\hat{H}$, where $\hat{P}$ projects onto the commutant of (i.e., the set of operators which commute with) $\{\hat{U}_b, \hat{U}_b^\dagger\}$ [23].

To eliminate $G_2(\hat{S}_{\mathbf{x}}\hat{J}_{\mathbf{x}} + \hat{S}_{\mathbf{y}}\hat{J}_{\mathbf{y}})$, while keeping $G_1\hat{S}_{\mathbf{z}}\hat{J}_{\mathbf{z}}$ we choose a $\hat{U}_b$ which commutes with $\hat{J}_{\mathbf{z}}$, but not with $\hat{J}_{\mathbf{x}}$ or $\hat{J}_{\mathbf{y}}$, namely, a π rotation about $\hat{J}_{\mathbf{z}}$, $\hat{U}_b = \exp[i\pi\hat{J}_{\mathbf{z}}]$. This leaves $\hat{J}_{\mathbf{z}}$ unchanged, but inverts $\hat{J}_{\mathbf{x}}$ and $\hat{J}_{\mathbf{y}}$. By the symmetry of $\hat{H}_{\mathrm{eff}}$, this is equivalent to inverting $\hat{S}_{\mathbf{x}}$ and $\hat{S}_{\mathbf{y}}$, which suggests a practical implementation: probe with pulses of alternating $\hat{S}_{\mathbf{x}}$, and define a meter variable taking into account the inversion of $\hat{S}_{\mathbf{y}}$.

We consider sequential interaction of the ensemble with a pair of pulses, with $\hat{S}_{\mathbf{x}}^{(1)} = -\hat{S}_{\mathbf{x}} = N_L/4p$. We define also the new meter variable $\hat{S}_{\mathbf{y}}^{(\mathrm{diff})} \equiv \hat{S}_{\mathbf{y}}^{(1)} - \hat{S}_{\mathbf{y}}^{(2)}$. We describe the atomic variables before, between, and after the two pulses with superscripts (in), (mid), and (out), respectively. We apply Eqs. (2)–(4) to find

$$\hat{J}_{\mathbf{z}}^{(\mathrm{mid})} = \hat{J}_{\mathbf{z}}^{(\mathrm{in})} - G_2\hat{S}_{\mathbf{x}}^{(1)}\hat{J}_{\mathbf{y}}^{(\mathrm{in})}, \tag{5}$$

$$\hat{J}_{\mathbf{y}}^{(\mathrm{mid})} = \hat{J}_{\mathbf{y}}^{(\mathrm{in})} - G_1\hat{S}_{\mathbf{z}}^{(1,\mathrm{in})}\hat{J}_{\mathbf{x}} - G_2\hat{S}_{\mathbf{x}}^{(1)}\hat{J}_{[\mathbf{x},\mathbf{y}]}^{(\mathrm{in})}, \tag{6}$$

$$\hat{S}_{\mathbf{y}}^{(1,\mathrm{out})} = \hat{S}_{\mathbf{y}}^{(1,\mathrm{in})} + G_1\hat{S}_{\mathbf{x}}^{(1)}\hat{J}_{\mathbf{z}}^{(\mathrm{in})}, \tag{7}$$

and

$$\hat{J}_{\mathbf{z}}^{(\mathrm{out})} = \hat{J}_{\mathbf{z}}^{(\mathrm{in})}, \tag{8}$$

$$\hat{S}_{\mathbf{y}}^{(\mathrm{diff,out})} = \hat{S}_{\mathbf{y}}^{(\mathrm{diff,in})} + 2G_1\hat{S}_{\mathbf{x}}^{(1)}\hat{J}_{\mathbf{z}}^{(\mathrm{in})} \tag{9}$$

plus terms in $G_1G_2\hat{S}_{\mathbf{x}}\hat{S}_{\mathbf{z}}\hat{J}_{\mathbf{x}}$, $G_2^2\hat{S}_{\mathbf{x}}^2\hat{J}_{[\mathbf{x},\mathbf{y}]}$, and $G_1G_2\hat{S}_{\mathbf{x}}^2\hat{J}_{\mathbf{y}}$ which become negligible in the limit of large p. The ideal QND form is recovered by the dynamical decoupling. The presence of the G_2 term can be detected by noise scaling properties. While in the ideal QND of Eqs. (8) and (9) the variance of the system variable is $\propto \hat{J}_{\mathbf{x}}$ giving a variance for the meter variable linear in $\hat{J}_{\mathbf{x}}$, for the imperfect QND of Eqs. (2)–(4) this is not the case: from Eq. (6), we see that $\hat{J}_{\mathbf{y}}$ acquires a backaction variance $\propto \hat{J}_{\mathbf{x}}^2$, which then is fed into the system variable by the G_2 term. This additional $\hat{J}_{\mathbf{x}}^2$ noise is also reflected in the meter variable, and provides a measurable indication of G_2.

We use the two-polarization decoupling technique to perform QND measurement on an ensemble of $\sim 10^6$ laser cooled ^{87}Rb atoms in the $F = 1$ ground state. In the atomic ensemble system, described in detail in Ref. [31], μs pulses interact with an elongated atomic cloud and are detected by a shot-noise-limited polarimeter. The experiment achieves projection-noise limited sensitivity, as calibrated against a thermal spin state [9].

The experimental sequence is shown schematically in Fig. 1. In each measurement cycle the atom number N_A is first measured by a dispersive atom-number measurement (DANM) [9]. A $\hat{J}_\mathbf{x}$-polarized coherent spin state (CSS) is then prepared and probed with pulses of alternating polarization to find the QND signal $\hat{S}_\mathbf{y} \equiv \Sigma_i \hat{s}^{(\mathrm{out})}_{\mathbf{y},i}(-1)^{i+1}$. Immediately after, $\langle \hat{J}_\mathbf{x} \rangle$ is measured to quantify depolarization of the sample and any atoms having made transitions to the $F = 2$ manifold are removed from the trap, reducing N_A for the next cycle and allowing a range of N_A to be probed on a single loading. This sequence of state preparation and probing is repeated 10 times for each loading of the trap. The trap is loaded 350 times to acquire statistics.

The optical dipole trap, formed by a weakly focused (52 μm) beam of a Yb:YAG laser at 1030 nm with 6 W of optical power, is loaded from a conventional two stage magneto-optical trap (MOT) during 4 s. Sub-Doppler cooling produces atom temperatures down to 25 μK as measured in the dipole trap [31]. In the DANM, we prepare a $\hat{J}_\mathbf{x}$-polarized CSS, i.e., all atoms in a coherent superposition of hyperfine states $|\uparrow / \downarrow\rangle \equiv |F = 1, m_F = \pm 1\rangle$, by optically pumping with vertically polarized light tuned to the transition $F = 1 \rightarrow F' = 1$, while also applying repumping on the $F = 2 \rightarrow F' = 2$ transition and a weak magnetic field along x to prevent spin precession. The atoms arrive to this dark state after scattering fewer than two photons on average. To measure $\langle \hat{J}_\mathbf{x} \rangle$, we send ten circularly polarized probe pulses, i.e., with $\langle \hat{S}_\mathbf{z} \rangle = N_L/2$, tuned 190 MHz to the red of the transition $F = 1 \rightarrow F' = 0$. Each pulse, of 1 μs duration, contains 2.6×10^6 photons and produces a signal $\langle \hat{S}_\mathbf{y} \rangle \propto G_2 \langle \hat{S}_\mathbf{z} \rangle \langle \hat{J}_\mathbf{x} \rangle$. The coherent state for the QND measurement is prepared in the same way, but in zero magnetic field.

To measure $\hat{J}_\mathbf{z}$, i.e., one-half the population difference between $|\uparrow\rangle$ and $|\downarrow\rangle$, we send probe pulses of either vertical $s_\mathbf{x} = n_L/2$ or horizontal $s_\mathbf{x} = -n_L/2$ polarization through the atomic sample and record their polarization rotation as $\hat{s}^{(\mathrm{out})}_{\mathbf{y},i}$. The probe light is detuned 600 MHz to the red of the transition $F = 1 \rightarrow F' = 0$. The number of individual probe pulses is $2p$ and the total number of probe photons $N_L = 2pn_L$.

In Fig. 2 we plot the measured noise versus atom number, which confirms the linear scaling characteristic of the QND measurement. The red squares indicate the variance $\mathrm{var}(\hat{S}_\mathbf{y})$ normalized to the optical polarization noise, measured in the absence of atoms. Independent measurements confirm the polarimetry is shot-noise limited in this regime. The black solid line is the expected projection-noise scaling $4\mathrm{var}(\hat{S}_\mathbf{y})/N_L = 1 + G_1^2 N_L \mathrm{var}(\hat{J}_\mathbf{z})$, calculated from the independently measured interaction strength G_1 and number of probe photons $N_L = 8 \times 10^8$. Spin polarized atoms with $\langle \hat{J}_\mathbf{z} \rangle = N_A/2$ and absorption imaging is used to calibrate G_1 [9]. The QND measurement achieves projection-noise limited sensitivity; i.e., the measurement noise is 5.7(6) dB below the projection noise.

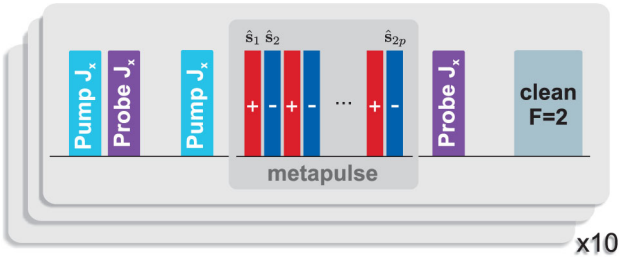

FIG. 1 (color online). Experimental sequence for projection-noise measurement. The CSS is prepared once and its magnitude $\langle \hat{J}_\mathbf{x} \rangle$ is measured. This serves as a measure of the spin polarization prior to the QND probing. We prepare the CSS a second time and assume it has the same spin polarization as in the first preparation. The state is probed with a train of pulses of alternating polarization. Measuring the spin polarization after the QND measurement tells us the amount of depolarization introduced in the QND probing. The QND probing scatters a non-negligible fraction of atoms into $F = 2$, which are removed from the trap with resonant light in order to reduce the number of atoms in the trap. The whole cycle is repeated 10 times during one trap loading.

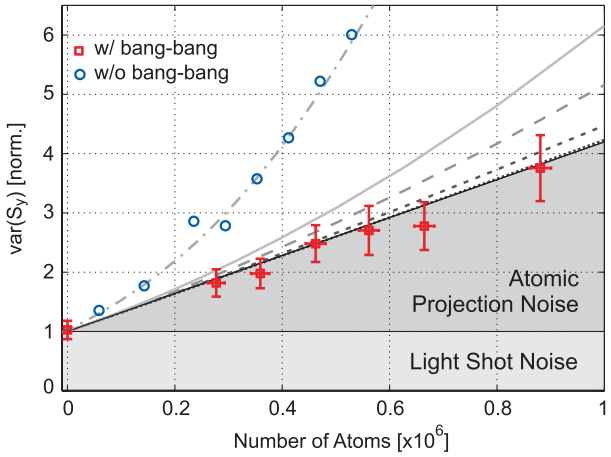

FIG. 2 (color online). Variance of polarimeter signal as a function of atom number, comparing naive probing, i.e., a single input polarization, to "bang-bang" dynamically decoupled probing of different orders p. Gray curves indicate simulation results for: naive probing (solid), and decoupled probing with $p = 1$ (widely dashed), $p = 2$ (dashed), and $p = 5$ (dotted). The black solid line shows the expected projection noise for $p \rightarrow \infty$, or the ideal QND interaction $G_2 = 0$. All curves are calculated using the independently measured interaction strength $G_1 = 1.27(5) \times 10^{-7}$ and have no free parameters. Red squares are measured data using dynamical decoupling with $p = 5$. Blue circles are measured data with naive probing, which show a quadratic scaling (dash-dotted line). Technical noise from laboratory fields dominates the naive probing results, and pushes them above the theoretical curve, while technical noise is suppressed in the two-polarization probing.

Also shown are results of covariance matrix calculations, following the techniques of reference [32], including loss and photon scattering. The scenarios considered include the naive QND measurement, i.e., with a single polarization, and the "bang-bang" or two-polarization QND measurement, with $p = 1, 2, 5$. These show a rapid decrease in the quadratic component with increasing p. This confirms the removal of G_2 due to the dynamical decoupling. Also included in these simulations is the term $\hat{S}_y\hat{J}_y$ which introduces noise into $\hat{J}_z$ proportional to $G_2^2 \mathrm{var}(\hat{S}_y)\langle\hat{J}_x\rangle^2$. For our experimental parameters this term leads to an increase of $\mathrm{var}(\hat{J}_z)$ of less then 2% and as noted above could be reduced with increased detuning.

The two-polarization probing also suppresses technical noise which would otherwise enter into $\hat{J}_z$ through the interaction $G_2(\hat{S}_x\hat{J}_x + \hat{S}_y\hat{J}_y)$. An imperfect preparation of the atomic and/or light state, e.g., $\langle\hat{J}_y\rangle \neq 0$ or $\langle\hat{S}_y\rangle \neq 0$, can causes classical noise in $\hat{J}_z$.

Using dynamical decoupling techniques, we have demonstrated optical quantum nondemolition measurement of a large-spin system. We first identify an often-overlooked impediment to this goal: the tensorial polarizability causes decoherence of the measured variable and prevents (naive) QND measurement of small ensembles. We then design an appropriate two-polarization probing strategy to cancel the tensorial components of the effective Hamiltonian and implement it with an ensemble of $\sim 10^6$ cold ^{87}Rb atoms. The dynamically decoupled QND measurement achieves a sensitivity 5.7(6) dB better than the projection-noise level. The technique will enable the use of large-spin ensembles in quantum metrology and quantum networking, and permit the QND measurement of exotic phases of large-spin condensed atomic gases.

We gratefully acknowledge fruitful discussions with Ivan H. Deutsch and Robert J. Sewell. This work was funded by the Spanish Ministry of Science and Innovation under the ILUMA project (Ref. FIS2008-01051) and the Consolider-Ingenio 2010 Project "QOIT."

*marco.koschorreck@icfo.es

[1] V. B. Braginsky and Y. I. Vorontsov, Sov. Phys. Usp. **17**, 644 (1975).
[2] J. P. Poizat, J. F. Roch, and P. Grangier, Ann. Phys. (Paris) **19**, 265 (1994).
[3] M. J. Holland, M. Collett, D. F. Walls, and M. D. Levenson, Phys. Rev. A **42**, 2995 (1990).
[4] A. Kuzmich, N. B. Bigelow, and L. Mandel, Europhys. Lett. **42**, 481 (1998).
[5] R. Ruskov, K. Schwab, and A. Korotkov, Phys. Rev. B **71**, 235407 (2005).
[6] J. Appel, P. J. Windpassinger, D. Oblak, U. Hoff, N. Kjaergaard, and E. S. Polzik, Proc. Natl. Acad. Sci. U.S.A. **106**, 10 960 (2009).
[7] M. H. Schleier-Smith, I. D. Leroux, and V. Vuletic, Phys. Rev. Lett. **104**, 073604 (2010).
[8] T. Takano, M. Fuyama, R. Namiki, and Y. Takahashi, Phys. Rev. Lett. **102**, 033601 (2009).
[9] M. Koschorreck, M. Napolitano, B. Dubost, and M. W. Mitchell, Phys. Rev. Lett. **104**, 093602 (2010).
[10] J. M. Geremia, J. K. Stockton, and H. Mabuchi, Phys. Rev. Lett. **94**, 203002 (2005).
[11] K. Eckert, O. Romero-Isart, M. Rodriguez, M. Lewenstein, E. S. Polzik, and A. Sanpera, Nature Phys. **4**, 50 (2008).
[12] K. Eckert, L. Zawitkowski, A. Sanpera, M. Lewenstein, and E. S. Polzik, Phys. Rev. Lett. **98**, 100404 (2007).
[13] T. Roscilde, M. Rodriguez, K. Eckert, O. Romero-Isart, M. Lewenstein, E. S. Polzik, and A. Sanpera, New J. Phys. **11**, 055041 (2009).
[14] J. M. Geremia, J. K. Stockton, and H. Mabuchi, Phys. Rev. A **73**, 042112 (2006).
[15] L. B. Madsen and K. Mølmer, Phys. Rev. A **70**, 052324 (2004).
[16] S. R. de Echaniz, M. W. Mitchell, M. Kubasik, M. Koschorreck, H. Crepaz, J. Eschner, and E. S. Polzik, J. Opt. B **7**, S548 (2005).
[17] G. A. Smith, S. Chaudhury, A. Silberfarb, I. H. Deutsch, and P. S. Jessen, Phys. Rev. Lett. **93**, 163602 (2004).
[18] D. V. Kupriyanov, O. S. Mishina, I. M. Sokolov, B. Julsgaard, and E. S. Polzik, Phys. Rev. A **71**, 032348 (2005).
[19] A. Kuzmich, L. Mandel, and N. B. Bigelow, Phys. Rev. Lett. **85**, 1594 (2000).
[20] B. Julsgaard, A. Kozhekin, and E. S. Polzik, Nature (London) **413**, 400 (2001).
[21] L. Viola and S. Lloyd, Phys. Rev. A **58**, 2733 (1998).
[22] L. Viola, E. Knill, and S. Lloyd, Phys. Rev. Lett. **82**, 2417 (1999).
[23] P. Facchi, S. Tasaki, S. Pascazio, H. Nakazato, A. Tokuse, and D. A. Lidar, Phys. Rev. A **71**, 022302 (2005).
[24] J. J. L. Morton, A. M. Tyryshkin, R. M. Brown, S. Shankar, B. W. Lovett, A. Ardavan, T. Schenkel, E. E. Haller, J. W. Ager, and S. A. Lyon, Nature (London) **455**, 1085 (2008).
[25] M. J. Biercuk, H. Uys, A. P. VanDevender, N. Shiga, W. M. Itano, and J. J. Bollinger, Nature (London) **458**, 996 (2009).
[26] C. Search and P. Berman, Phys. Rev. Lett. **85**, 2272 (2000).
[27] J. Taylor, P. Cappellaro, L. Childress, L. Jiang, D. Budker, P. Hemmer, A. Yacoby, R. Walsworth, and M. D. Lukin, Nature Phys. **4**, 810 (2008).
[28] R. S. Minns, M. R. Kutteruf, H. Zaidi, L. Ko, and R. R. Jones, Phys. Rev. Lett. **97**, 040504 (2006).
[29] S. Damodarakurup, M. Lucamarini, G. D. Giuseppe, D. Vitali, and P. Tombesi, Phys. Rev. Lett. **103**, 040502 (2009).
[30] E. Fraval, M. Sellars, and J. Longdell, Phys. Rev. Lett. **92**, 077601 (2004).
[31] M. Kubasik, M. Koschorreck, M. Napolitano, S. R. D. Echaniz, H. Crepaz, J. Eschner, E. S. Polzik, and M. W. Mitchell, Phys. Rev. A **79**, 043815 (2009).
[32] M. Koschorreck and M. W. Mitchell, J. Phys. B **42**, 195502 (2009).